

Instability of regularized 4D charged Einstein-Gauss-Bonnet de-Sitter black holes*

Peng Liu(刘鹏)[†] Chao Niu(牛超)[‡] Cheng-Yong Zhang(张承勇)[§]

Department of Physics and Siyuan Laboratory, Jinan University, Guangzhou 510632, China

Abstract: We studied the instability of regularized 4D charged Einstein-Gauss-Bonnet de-Sitter black holes under charged scalar perturbations. The unstable modes satisfy the superradiant condition, but not all of the modes satisfying the superradiant condition are unstable. The instability occurs when the cosmological constant is small and the black hole charge is not too large. The Gauss-Bonnet coupling constant further destabilizes black holes when both the black hole charge and the cosmological constant are small and further stabilizes black holes when the black hole charge is large.

Keywords: black hole, Einstein-Gauss-Bonnet, instability

DOI: 10.1088/1674-1137/abcd2d

I. INTRODUCTION

It is known that general relativity should be modified from the viewpoints of both theory and observations. For example, general relativity cannot be renormalized and cannot explain the dark side of the universe. In contrast, the Lovelock theorem states that, in the four dimensional vacuum spacetime, general relativity with the cosmological constant is a unique metric theory of gravity with second order equations of motion and covariant divergence-free [1]. Beyond general relativity, one must consider higher dimensional spacetimes, add extra fields, allow higher order derivatives of metrics, or even abandon the Riemannian geometry. Various modified gravity theories have been proposed [2].

By rescaling the GB coupling constant in a special way, a regularized 4D GB black hole solution was found recently [3]. This work provides a novel classical 4D gravity theory and has inspired many studies, including those on regularized black hole solutions [4-23], perturbations [24-35], shadow and geodesics [36-41], thermodynamics [42-47], and other aspects [48-51]. It should be mentioned that 4D EGB gravity was found to be inconsistent based on the theory proposed in [3]. Fortunately, some proposals have been raised to circumvent the issues of 4D EGB gravity, including adding an extra degree of freedom to the theory [18-23] or breaking the temporal diffeomorphism invariance [52, 53], where a well-defined theory was formulated. In contrast, while the 4D EGB

gravity formulated in [3] may be problematic at the level of action or equations of motion, the spherically symmetric black hole solution derived in [3] can be obtained from conformal anomaly and quantum corrections [54-65] as well as from the Horndeski theory [18-23], which means the spherically symmetric black hole solution itself is meaningful and worth studying.

The regularized black hole solution has some remarkable properties. Its singularity at the center is timelike. The gravitational force near the center is repulsive, and the free infalling particles cannot reach the singularity [3]. One may expect that the regularized black hole solution would also show some novel properties with respect to perturbations, and some related studies have been reported [24-32, 34]. The study of the stability of black holes is an active area in black hole physics. It can be used for extracting the black hole parameters such as its mass, charge, and angular momentum. Black hole stability is also related to gravitational waves, black hole thermodynamics, the information paradox, and holography [57, 58]. Among these studies, black hole stability in the asymptotic de Sitter (dS) spacetime is intriguing. For example, spontaneous scalarization of Kerr-dS black holes in the scalar-tensor theory behaves very differently from that for asymptotically flat spacetimes under perturbations [59]. The 4D Reissner-Nordström-de Sitter (RN-dS) black hole may violate strong cosmic censorship [60-63]. Higher dimensional RN-dS and Gauss-Bonnet-de Sitter (GB-dS) black holes are unstable [64-68].

Received 9 September 2020; Accepted 22 October 2020; Published online 8 December 2020

* Supported by the National Natural Science Foundation of China (11847055, 11905083, 11805083, 11947067)

[†] E-mail: phylp@jnu.edu.cn

[‡] E-mail: niuchaophy@gmail.com

[§] E-mail: zhangcy@email.jnu.edu.cn

©2021 Chinese Physical Society and the Institute of High Energy Physics of the Chinese Academy of Sciences and the Institute of Modern Physics of the Chinese Academy of Sciences and IOP Publishing Ltd

A quite surprising and still not very well understood result was discovered in [69-71], where it was shown that the RN-dS black hole is unstable under charged scalar perturbations. Such instability satisfies the superradiance condition [72]. However, only the monopole $l=0$ suffers from this instability. Higher multipoles are stable. This is distinct from superradiance. The underlying mechanism may be understood using the tools of nonlinear analysis, as was partially shown recently [63]. In this paper, we consider the instability of the regularized 4D charged EGB black hole in the asymptotic dS spacetime, under charged scalar perturbations. We demonstrate that the behavior is very different from the case of the asymptotic flat spacetime that was considered in [34]. The GB coupling constant plays a more subtle role here.

The paper is organized as follows. Sec. II describes the regularized 4D EGB-RN-dS black hole and gives a reasonable parametric region. Sec. III presents the charged scalar perturbation equations. Sec. IV describes the numerical method we used and presents the results for quasinormal modes (QNMs). Sec. V contains the summary and discussion of the study.

II. THE 4D CHARGED EGB-DS BLACK HOLE

The 4D spherical symmetric EGB black hole in the electrovacuum dS spacetime can be written as [4]

$$ds^2 = -f(r)dt^2 + \frac{1}{f(r)}dr^2 + r^2(d\theta^2 + \sin^2\theta d\phi^2), \quad (1)$$

where the metric function is

$$f(r) = 1 + \frac{r^2}{2\alpha} \left(1 - \sqrt{1 + 4\alpha \left(\frac{M}{r^3} - \frac{Q^2}{r^4} + \frac{\Lambda}{3} \right)} \right), \quad (2)$$

and the gauge potential is

$$A = -\frac{Q}{r} dt. \quad (3)$$

Here, M is the black hole mass, Q is the black hole charge, and Λ the positive cosmological constant. When $\alpha \rightarrow 0$, this solution converges to that for the RN-dS black hole. As $r \rightarrow \infty$, the asymptotic dS spacetime with an effective positive cosmological constant is obtained. Note that solution (1) coincides formally with those obtained from the Horndeski theory [18-23] and those obtained using conformal anomaly and quantum corrections [52, 53].

The GB coupling constant α can be either positive or negative. In an appropriate parametric region, the solution has three horizons: the inner horizon r_- , the event

horizon r_+ , and the cosmological horizon r_c . For negative α , the metric function may not be real in the small r region. However, since we are only interested in the region between r_+ and r_c , we allow negative α in this work. For convenience, hereafter, we fix the black hole event horizon as $r_+ = 1$. Then, the mass parameter can be expressed as

$$M = 1 - \frac{\Lambda}{3} + Q^2 + \alpha. \quad (4)$$

Note that, to ensure $f(1) = 0$, we must have $\alpha > -\frac{1}{2}$. The parametric region in which the black hole event horizon r_+ and the cosmological horizon r_c are allowed can be determined by requiring $f'(r_+) > 0$, implying that the black hole temperature is positive. This leads to

$$Q^2 + \alpha + \Lambda < 1. \quad (5)$$

This formula is very similar to the neutral case [33]. The parametric region is shown in Fig. 1.

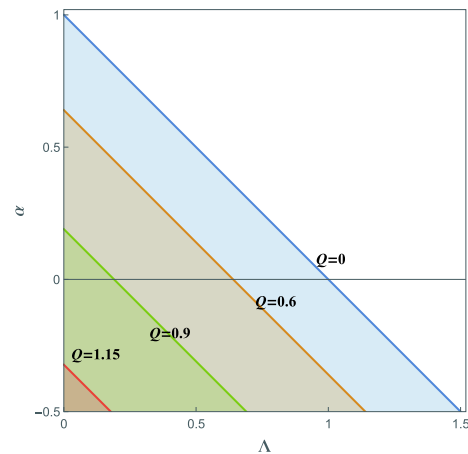


Fig. 1. (color online) The parametric region that allows the event horizon r_+ and cosmological horizon r_c . The region is bounded by $Q^2 + \alpha + \Lambda < 1$, $-0.5 < \alpha$, $\Lambda > 0$, and $Q > 0$. As Q increases, the allowed region for (Λ, α) shrinks. The extremal value of $Q = \sqrt{3/2}$.

III. THE CHARGED SCALAR PERTURBATION

It is known that fluctuations of order $O(\epsilon)$ in the scalar field in a given background induce changes in the spacetime geometry of order $O(\epsilon^2)$ [72]. To the leading order, we can study perturbations for a fixed background geometry. Let us consider a massless charged scalar field ψ on background (1). Its equation of motion is

$$0 = D^\mu D_\mu \psi \equiv g^{\mu\nu} (\nabla_\mu - iqA_\mu) (\nabla_\nu - iqA_\nu) \psi, \quad (6)$$

where q is the scalar charge, and ∇_μ is the covariant derivative. For a generic background, we can take the following decomposition

$$\psi = \sum_{lm} \int d\omega e^{-i\omega t} \frac{\Psi(r)}{r} Y_{lm}(\theta, \phi). \quad (7)$$

Here, $Y_{lm}(\theta, \phi)$ is the spherical harmonics on the two sphere S^2 . The angular part and the radial part of the perturbation Eq. (6) decouple. What we are interested in is the radial part, which can be written in the Schrödinger-like form

$$0 = \frac{\partial^2 \Psi}{\partial r_*^2} + \left(\omega^2 - \frac{2qQ}{r} \omega - V_{\text{eff}} \right) \Psi, \quad (8)$$

where the tortoise coordinate $dr_* = dr/f$ is introduced. The effective potential reads

$$V_{\text{eff}} = -\frac{q^2 Q^2}{r^2} + f \left(\frac{l(l+1)}{r^2} + \frac{\partial_r f}{r} \right). \quad (9)$$

Unlike the case of the asymptotic flat spacetime, where only one potential barrier appears between r_+ and r_c , here, a negative effective potential well may appear between r_+ and r_c . We will show that this potential well plays an important role in the instability of charged EGB-dS black holes under perturbations.

The radial equation exhibits the following asymptotic behavior near the horizons.

$$\Psi \rightarrow \begin{cases} e^{-i(\omega - \frac{qQ}{r_+})r_*} \sim (r - r_+)^{-\frac{i}{2\kappa_+}(\omega - \frac{qQ}{r_+})}, & r \rightarrow r_+, \\ e^{i(\omega - \frac{qQ}{r_c})r_*} \sim (r - r_c)^{-\frac{i}{2\kappa_c}(\omega - \frac{qQ}{r_c})}, & r \rightarrow r_c. \end{cases} \quad (10)$$

Here, $\kappa_+ = \frac{1}{2f'(r_+)}$ is the surface gravity on the event horizon, and $\kappa_c = -\frac{1}{2f'(r_c)}$ is the surface gravity on the cosmological horizon. This asymptotic solution corresponds to the ingoing boundary condition near the event horizon and outgoing boundary condition near the cosmological horizon. The system is dissipative, and the frequency of perturbations is determined by the composition of QNMs. For a specific boundary condition (10), the radial Eq. (8) can be solved as an eigenvalue problem. Only some discrete eigenfrequencies ω satisfy both the radial equation and the boundary condition. The eigenfrequency can be written as $\omega = \omega_R + i\omega_I$. When the imaginary part $\omega_I > 0$, the amplitude of the perturbation will increase exponentially, implying that the black hole is unstable at least with respect to linear perturbations.

IV. THE INSTABILITY OF THE 4D CHARGED EGB-DS BLACK HOLE

The radial Eq. (8) with boundary conditions specified by (10) is generally difficult to solve analytically, except for a few cases, such as the pure anti-dS ((A)dS) spacetime, the Nariai spacetime, and massless topological black holes [57, 58]. In general, approximations or numerical methods are required. Various numerical methods for QNM calculations have been developed, such as the Wentzel-Kramers-Brillouin (WKB) method, the shooting method, the continued fraction method, and the Horowitz-Hubeny method [57, 58]. Not all of these methods have high accuracy and efficiency in the charged case [73]. In this work, we adopted the asymptotic iteration method [74, 75]. In addition, we validate our results using asymptotic iteration methods with time evolution.

A. The asymptotic iteration method (AIM)

The AIM was originally developed for solving the eigenvalues of homogeneous second order ordinary derivative functions [76, 77]. Later, it was used for observing QNMs of black holes in the asymptotic flat or (A)dS spacetimes [74, 75]. Let us first introduce an auxiliary variable

$$\xi = \frac{r - r_+}{r_c - r_+}. \quad (11)$$

It ranges from 0 to 1 as r runs from the event horizon to the cosmological horizon. The radial Eq. (8) then becomes

$$0 = \frac{\partial^2 \Psi}{\partial \xi^2} \left(\frac{f}{r_c - r_+} \right)^2 + \frac{\partial \Psi}{\partial \xi} \frac{f \partial_\xi f}{(r_c - r_+)^2} + \left[\left(\omega - \frac{qQ}{(r_c - r_+) \xi + r_+} \right)^2 - f \left(\frac{l(l+1) + \left(\xi + \frac{r_+}{r_c - r_+} \right) \partial_\xi f}{[(r_c - r_+) \xi + r_+]^2} \right) \right] \Psi. \quad (12)$$

The above equation is in general difficult to solve analytically; thus, we use numerical methods. In terms of ξ , the asymptotic solution near the horizons can be written as

$$\Psi \rightarrow \begin{cases} \xi^{-\frac{i}{2\kappa_+}(\omega - \frac{qQ}{r_+})}, & \xi \rightarrow 0, \\ (\xi - 1)^{-\frac{i}{2\kappa_c}(\omega - \frac{qQ}{r_c})}, & \xi \rightarrow 1. \end{cases} \quad (13)$$

Then, we can write the full solution of Eq. (12) satisfying the asymptotic behavior (13), as follows:

$$\Psi = \xi^{-\frac{i}{2\kappa_+}(\omega - \frac{qQ}{r_+})} (\xi - 1)^{\frac{i}{2\kappa_c}(\omega - \frac{qQ}{r_c})} \chi(\xi). \quad (14)$$

Here, $\chi(\xi)$ is a regular function of ξ in the interval $(0, 1)$, and it obeys the following homogeneous second order differential equation

$$\frac{\partial^2 \chi}{\partial \xi^2} = \lambda_0(\xi) \frac{\partial \chi}{\partial \xi} + s_0(\xi) \chi, \quad (15)$$

in which the coefficients are

$$-\lambda_0(\xi) = \frac{i\left(\omega - \frac{qQ}{r_c}\right)}{(\xi - 1)\kappa_c} - \frac{i\left(\omega - \frac{qQ}{r_+}\right)}{\kappa_+ \xi} + \frac{f'(\xi)}{f(\xi)}, \quad (16)$$

$$\begin{aligned} -s_0(\xi) = & -\frac{(r_c - r_+)((\xi r_c - \xi r_+ + r_+)f'(\xi) + l(l+1)(r_c - r_+))}{f(\xi)((\xi - 1)r_+ - \xi r_c)^2} - \frac{\left(\omega - \frac{qQ}{r_c}\right)\left(\frac{\omega r_c - qQ}{2\kappa_c r_c} + i\right)}{2(\xi - 1)^2 \kappa_c} \\ & + \frac{\left(\omega - \frac{qQ}{r_+}\right)\left(\frac{qQ - r_+ \omega}{2\kappa_+ r_+} + i\right)}{2\kappa_+ \xi^2} + \frac{\left(\omega - \frac{qQ}{r_+}\right)\left(\omega - \frac{qQ}{r_c}\right)}{2\kappa_+(\xi - 1)\xi \kappa_c} \\ & + \frac{if'(\xi)\left(\omega - \frac{qQ}{r_c}\right)}{2(\xi - 1)\kappa_c f(\xi)} - \frac{if'(\xi)\left(\omega - \frac{qQ}{r_+}\right)}{2\kappa_+ \xi f(\xi)} + \frac{(r_c - r_+)^2 \left(\omega - \frac{qQ}{\xi r_c - \xi r_+ + r_+}\right)^2}{f(\xi)^2}. \end{aligned} \quad (17)$$

The coefficients $\lambda_0(\xi)$ and $s_0(\xi)$ are regular functions of ξ in the interval $(0, 1)$. Differentiating (15) with respect to ξ iteratively leads to an $(n+2)$ -th order differential equation

$$\chi^{(n+2)} = \lambda_n(\xi) \chi'(\xi) + s_n(\xi) \chi(\xi), \quad (18)$$

where the coefficients are determined iteratively, as follows:

$$\begin{aligned} \lambda_n(\xi) &= \lambda'_{n-1}(\xi) + s_{n-1}(\xi) + \lambda_0(\xi) \lambda_{n-1}(\xi), \\ s_n(\xi) &= s'_{n-1}(\xi) + s_0(\xi) \lambda_{n-1}(\xi). \end{aligned} \quad (19)$$

Expanding the coefficient functions around a regular point $\xi = \xi_0$,

$$\begin{aligned} \lambda_n(\xi) &= \sum_{j=0}^{\infty} c_n^j (\xi - \xi_0)^j, \\ s_n(\xi) &= \sum_{j=0}^{\infty} d_n^j (\xi - \xi_0)^j, \end{aligned} \quad (20)$$

in which the expansion coefficients c_n^j and d_n^j are functions of ω , and the iterative equations give

$$c_n^j = (j+1)c_{n-1}^{j+1} + d_{n-1}^j + \sum_{k=0}^j c_0^k c_{n-1}^{j-k}, \quad (21)$$

$$d_n^j = (j+1)d_{n-1}^{j+1} + \sum_{k=0}^j d_0^k c_{n-1}^{j-k}. \quad (22)$$

For sufficiently large n , the cutoff of the iteration in the AIM is given by

$$\frac{s_n(\xi)}{\lambda_n(\xi)} = \frac{s_{n-1}(\xi)}{\lambda_{n-1}(\xi)}, \quad (23)$$

which leads to the following expression, in terms of the expansion coefficients:

$$d_n^0 c_{n-1}^0 = d_{n-1}^0 c_n^0. \quad (24)$$

The QNMs ω can be worked out by solving this equation. We vary the iteration times and the expansion point to ensure the reliability of the results. The results are also checked by using other auxiliary variables such as $\xi = 1 - \frac{r_+}{r}$ or $\xi = \left(1 - \frac{r_+}{r}\right) / \left(1 - \frac{r_+}{r_c}\right)$. Except for some extremal cases ($\Lambda \rightarrow 0$ or when the black hole becomes extremal), they coincide well. Hereafter, we set $q = 1$ for convenience.

B. The eigenfrequencies of the charged scalar perturbation

Let us first study the effects of the black hole charge Q on the fundamental modes of QNMs. The results are shown in Fig. 2. In the left panel, we see that ω_R increases with Q almost linearly. The slope is steeper for larger Λ and α . In the right panel, ω_I increases for small Q and then decreases for larger Q . For sufficiently large Q , the black hole becomes stable. When Q is small, ω_I increases with increasing α . This behavior is similar to the case of the asymptotic flat spacetime [34]. However, when Q is large, ω_I decreases with increasing ω_I . This

should be contrasted with the result for the asymptotic flat spacetime. It implies that the positive GB coupling constant can destabilize the black hole when the black hole charge Q is small, whereas it stabilizes the black hole at large Q . Note further that, regardless of the values of Λ, α considered, when $Q \rightarrow 0$, both ω_R and ω_I tend to 0 from above. This implies that weakly charged black holes in the dS spacetime are always unstable. The existence of α does not change this phenomenon qualitatively.

Now, we study the effects of α on the fundamental modes in more detail. Fig. 3 shows the real part of the fundamental modes ω_R , for $Q = 0.1$ and $Q = 0.4$. For fixed Q , the real part ω_R increases almost linearly with α and Λ . Combining the results from Fig. 2, we conclude that $\omega_R \propto \alpha \Lambda Q$.

The behavior of the imaginary part of the fundamental modes ω_I is more interesting. In Fig. 4, we show the cases for $Q = 0.1$ and $Q = 0.4$. From the left and right panels, we see that ω_I increases with small Λ and decreases with larger Λ . The effect of α on ω_I is subtle and relevant to Λ and Q . When both Q and Λ are small (left upper panel), ω_I increases with α . For small Q and larger Λ (right upper panel), ω_I increases with α first and then decreases with α . For larger Q (lower panels), ω_I decreases with α . This phenomenon is very different from the case of the asymptotic flat spacetime [34], where α roughly increases ω_I . This implies that the positive GB

coupling constant α can suppress the black hole instability. As α increases, it can even change the qualitative behavior of a black hole under a perturbation and can render an unstable black hole stable.

The instability we found here is reminiscent of superradiance. However, the present case is quite subtle. Using a method similar to that in [34, 70], one can show that the superradiance occurs only when

$$\frac{qQ}{r_+} > \omega > \frac{qQ}{r_c}. \quad (25)$$

Although the unstable modes encountered in our study indeed satisfy (25), it is observed that some oscillation frequencies corresponding to stable modes also are in the range determined by (25) (see Table 1 for evidence). In fact, as shown in [34, 70], the superradiant condition is the necessary but not sufficient condition for instability. The precise mechanism of the instability found here should be studied better and will be addressed in Sec. V.

C. Evolution of the perturbation field

We also directly compute the time-evolution of the perturbation field ψ to further reveal the instability of the 4D charged EGB-dS black hole. For the time evolution, the Schrödinger-like equation becomes

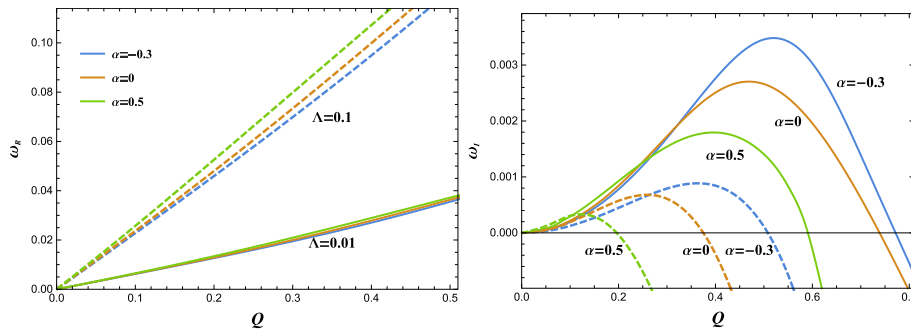


Fig. 2. (color online) The real part (left) and the imaginary part (right) of the fundamental modes of the QNMs, for $l = 0$. The solid lines are for $\Lambda = 0.01$, while the dashed lines are for $\Lambda = 0.1$.

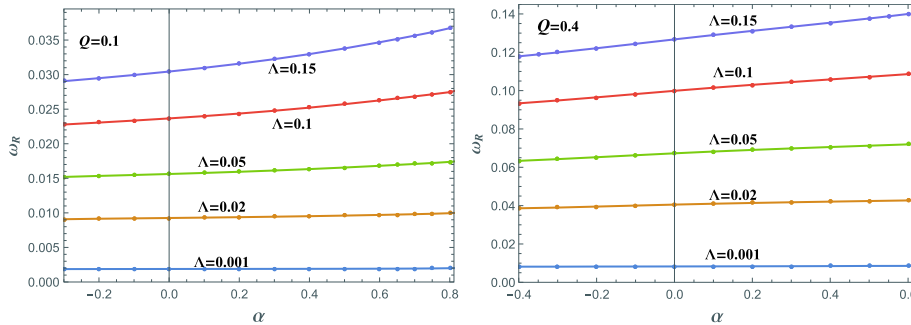


Fig. 3. (color online) The real part of the fundamental modes of the QNMs, for $l = 0$. The left panel is for $Q = 0.1$, while the right panel is for $Q = 0.4$.

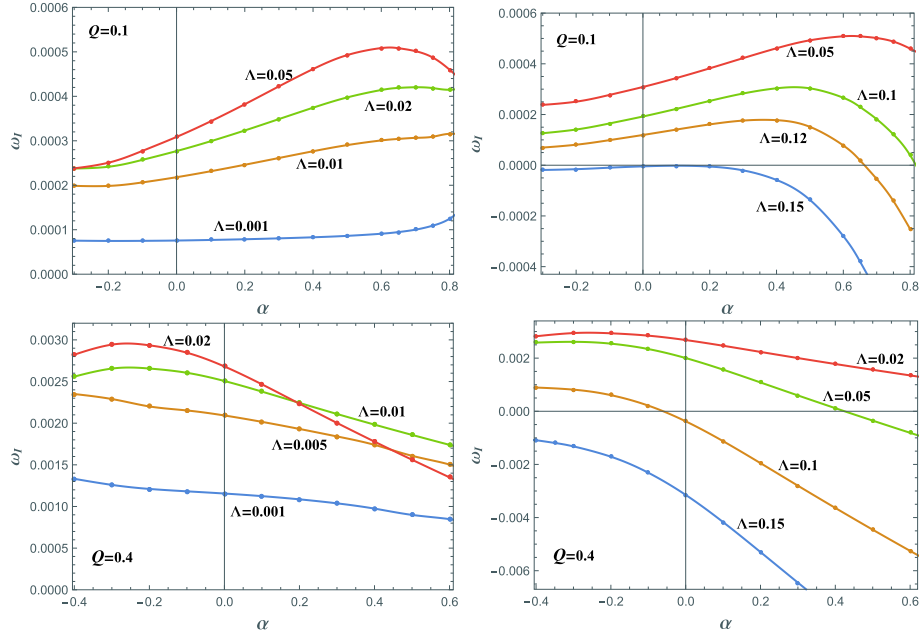


Fig. 4. (color online) The imaginary part of the fundamental modes of the QNMs, for $l = 0$. The upper panel is for $Q = 0.1$, while the lower panel is for $Q = 0.4$. The left panel shows the results for small Λ , while the right panel shows the results for larger Λ .

Table 1. The fundamental modes for $Q = 0.1$, $\Lambda = 0.12$, and $l = 0$, corresponding to the orange line in the upper right panel of Fig. 4. The last column is the imaginary part of the frequency extracted from the time evolution.

α	$\frac{qQ}{r_+}$	$\frac{qQ}{r_c}$	ω (AIM)	ω_I (time domain)
0.5	0.1	0.0244042	0.0290311+0.0001514i	0.0001515
0.6	0.1	0.0248557	0.0297114+0.0000779i	0.0000780
0.65	0.1	0.0250987	0.0300692+0.0000191i	0.0000192
0.7	0.1	0.0253547	0.0304355-0.0000541i	-0.0000547
0.75	0.1	0.0256252	0.0308094-0.0001400i	-0.0001390

$$-\frac{\partial^2 \Psi}{\partial r^2} - \frac{2iqQ}{r} \frac{\partial \Psi}{\partial t} + \frac{\partial^2 \Psi}{\partial r_*^2} - V(r)\Psi = 0, \quad (26)$$

In order to compute the time evolution of ψ , we adopt the discretization approach introduced in [69]. The reliability of this numerical method can be verified by the convergence of computations when increasing the sampling density. We impose the following initial profile:

$$\begin{cases} \Psi(r_*, t) = 0, & t < 0, \\ \Psi(r_*, t) = \exp\left[-\frac{(r_* - a)^2}{2b^2}\right], & t = 0. \end{cases} \quad (27)$$

Eq. (26) is discretized in the (r_*, t) plane. In addition, we set $\Delta t/\Delta r_* = 0.5$, to satisfy the von Neumann stability conditions. Unlike some other analytical models where r_* can be solved analytically, here, $r_*(r)$ can only be obtained numerically; $r_*(r)$ diverges as $\lim_{r \rightarrow r_*} \rightarrow -\infty$ and $\lim_{r \rightarrow r_c} \rightarrow \infty$; hence, the error of numerical $r_*(r)$ can be very large in the near horizon region. Therefore, we intro-

duce a cutoff ϵ for solving the $r_*(r)$ relation by solving the following system expression:

$$r_*'(r) = 1/f(r), \quad r_*(r_h + \epsilon) = 0, \quad \text{with } r \in [r_h + \epsilon, r_c - \epsilon]. \quad (28)$$

Usually, the cutoff ϵ should not be too small; otherwise, it will lead to a significant error in the resultant $r_*(r)$.

To obtain the late time evolution of the perturbation, we need to solve a large range of r_* . Since $1/f$ tends to diverge when $r \rightarrow r_h$ and $r \rightarrow r_c$, in the near horizon region, $r_*(r)$ can be extracted analytically. A direct solution is to expand $1/f(r)$ with respect to r_h , because the horizon requires that $1/f(r) \sim 1/(r - r_h)$. However, this direct expansion can lead to very large numerical errors. A better solution is to expand $f(r)$ with respect to r_h and then obtain the expansion of $1/f$ in terms of the expansion coefficients of $f(r)$. After solving the analytical expansion coefficients, one may glue the analytical expan-

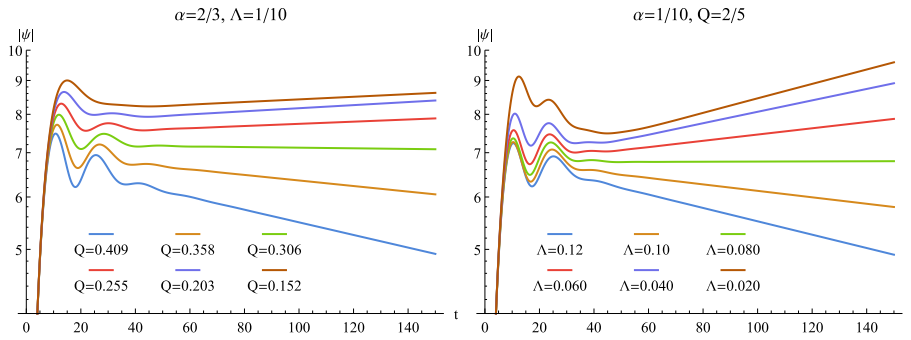


Fig. 5. (color online) Left panel: the time evolution of $|\psi(r_*, t)|$ at $\alpha = 2/3$, $\Lambda = 1/10$, where the different curves correspond to the different values of Q . Right panel: the time evolution of $|\psi(r_*, t)|$ at $\alpha = 1/10$, $Q = 2/5$, where the different curves correspond to the different values of Λ . For both plots we set $a = 88.4216$, $b = 1/10$.

sion in the near horizon region and the numerical solution of $r_*(r)$ in $r \in [r_h + \epsilon, r_c - \epsilon]$. In this way, one may obtain a very large range of r_* , and long-time evolution can be realized.

We show two examples of $|\psi(t)|$ in the log plot in Fig. 5, from which we can see that $\ln|\psi|$ linearly depends on t at later times. From the left panel of Fig. 5, when Q is small, the system is unstable ($\ln|\psi|$ linearly decreases with t), while for large values of Q , the system becomes stable ($\ln|\psi|$ linearly grows with t). This is in accordance with previous results of the frequency analysis (see the right panel of Fig. 2). From the right panel of Fig. 5, we see that when Λ is small, the system is unstable ($\ln|\psi|$ linearly increases with t), while for large values of Λ , the system becomes stable ($\ln|\psi|$ linearly decreases with t). This is in accordance with previous results of the frequency analysis (see the bottom right panel of Fig. 4).

It is also important to verify the validity of the AIM with respect to the time evolution. There are comprehensive methods for extracting frequencies from the perturbations' time-domain profiles, such as the Prony method used in [69]. Here, we extract ω_I by computing $\partial_t \ln(|\psi|)$ for later times and compare the results with those obtained using the AIM. This simple process only allows to extract the imaginary part of the dominant mode and may not be sufficiently accurate when QNMs are close to each other. However, it is sufficiently good for the purposes of our current analysis. We provide the comparison in Table 1 (see the last two columns), from which we can see that all of the time evolution results perfectly agree with those of the AIM.

Finally, we show the unstable region of the charged EGB-dS black hole under charged scalar perturbation in Fig. 6. The black hole is unstable only when Λ and Q are not too large. As Λ or Q increases, the black hole becomes less unstable. For positive α , the unstable region shrinks. For negative α , the unstable region widens. Although we do not show the results for $\Lambda \rightarrow 0$ owing to the limitation of our numerical method, we can expect that there should be sudden drops, since we have found that there is no instability for the asymptotic flat charged EGB

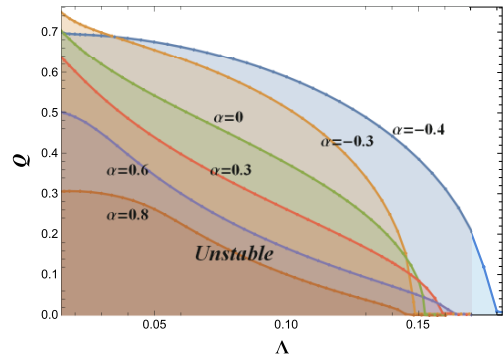


Fig. 6. (color online) The unstable region of the charged EGB-dS black hole under a charged scalar perturbation. The shadows under the constant α lines are the corresponding unstable regions. Here, $q = 1$.

black holes under charged scalar perturbations [34]. This phenomenon was also disclosed for RN-dS black holes in [70].

D. Effective potential

Now let us take a look at the effective potential when $l = 0$. In the left panel of Fig. 7, we see that there is a negative potential well between r_+ and r_c . This potential well is the key point for the occurrence of instability. However, the negative effective potential does not guarantee $\omega_I > 0$. For example, the case $\alpha = 0.8$ has a negative potential well, but $\omega_I < 0$. Thus, the existence of a negative potential well can be viewed as the necessary but not sufficient condition for instability [78]. In the right panel of Fig. 7, the potential well disappears for larger α . The perturbation wave can be easily absorbed by the black hole, and the corresponding background becomes stable with respect to charged scalar perturbations. Note that the positive cosmological constant is crucial here for creating the necessary potential well.

Now, let us consider the eigenfrequencies of the charged scalar perturbation when $l = 1$. The fundamental modes are shown in Fig. 8. The left panel shows that the real part $\omega_R \propto Q$ still exists for higher l . However, α very

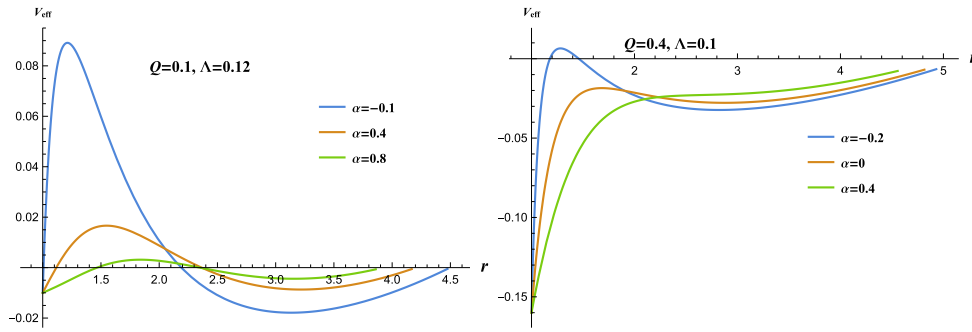


Fig. 7. (color online) The effective potential when $l = 0$. The left and right plots correspond to the orange lines in the upper right and lower right panels of Fig. 4, respectively.

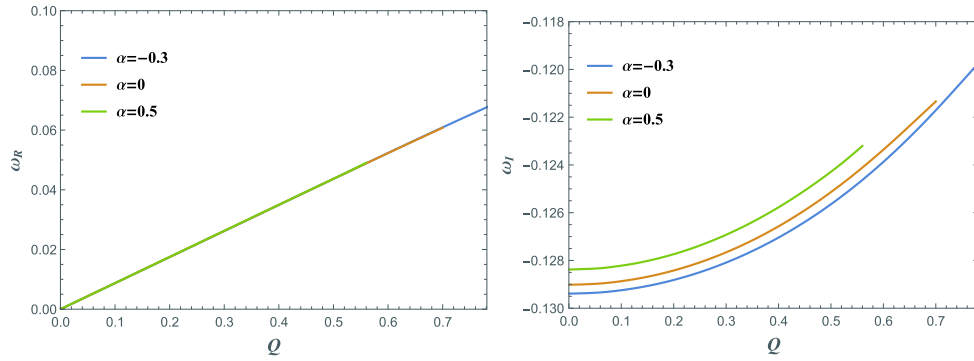


Fig. 8. (color online) The real part (left) and imaginary part (right) of the fundamental modes when $l = 1$. Here, $\Lambda = 0.05$. The results for other Λ values are similar.

weakly affects ω_R . All of the fundamental modes have $\omega_R < \frac{qQ}{r_c}$ beyond the superradiant condition. The results in the left panel are different from those in Fig. 2. Here, ω_I increases with Q and α monotonically. Note that all of the modes are stable now.

The stability for the higher l values can be explained using the effective potential, as shown in Fig. 9. There is only one potential barrier and there are no potential wells to accumulate the energy for triggering instability.

A detailed time evolution for $l \neq 0$ is shown in Fig. 10. From these two panels, we see that the perturbations indeed decay in the long term, and larger l values yield a more significant decay of ψ ; hence, no instability occurs for higher values of l .

V. SUMMARY AND DISCUSSION

We studied the instability of charged 4D EGB-dS black holes with respect to charged massless scalar perturbations. This instability satisfies the superradiant condition. However, not all of the modes satisfying the superradiant condition are unstable. The precise mechanism of this instability is not well understood. Nevertheless, the positive cosmological constant Λ should play a crucial role. The instability occurs when the cosmological constant is small. This is reminiscent of the Gregory-Laflamme instability [79] since there exists a hierarchy

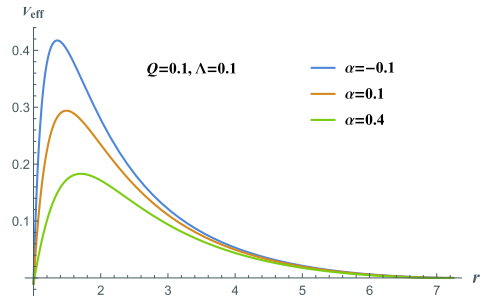


Fig. 9. (color online) The effective potential when $l = 1$. The results for other Q, Λ values are similar.

between the black hole event horizon and the cosmological horizon. The instability here is different from the " Λ instability" found in [35, 64-68], which occurs when the black hole charge and the cosmological constant are large.

We analyzed this instability from the viewpoint of the effective potential. Higher l has only one potential barrier beyond the event horizon. The perturbation dissipates and does not lead to instability. The monopole $l = 0$ has a negative potential well between the event horizon and cosmological horizon, which can accumulate the energy necessary for triggering the instability. But the negative potential well is just the necessary but not sufficient condition for the instability.

Unlike the case of the asymptotic flat spacetime, the

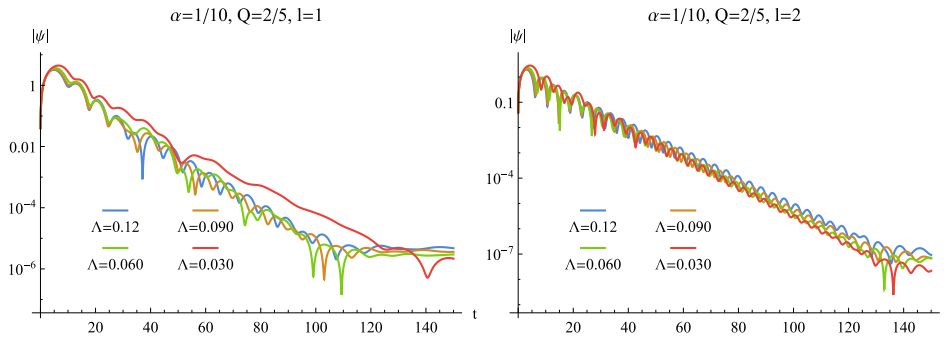


Fig. 10. (color online) The time evolution of $|\psi(r_*, t)|$ in the log plot at $\alpha = 1/10, Q = 2/5, a = 88.4216, b = 1/10$, and $q = 1$, where the different curves in both panels correspond to the different values of Λ . The left and the right panels show the results for $l = 1$ and $l = 2$, respectively.

effect of the GB coupling constant α on the perturbation is relevant to the black hole charge and cosmological constant. It makes an unstable black hole more unstable when both the black hole charge and cosmological constant are small and makes a stable black hole more stable when the black hole charge is large. Weakly charged black holes in the dS spacetime are always unstable. The existence of α does not change this phenomenon qualitatively. However, α can change the qualitative behavior when the black hole charge is large and make unstable black holes stable. We show that the unstable region of (Λ, Q) shrinks for positive α and enlarges for negative α . Unfortunately, our results are not sufficiently accurate for $\Lambda \rightarrow 0$, owing to the limitation of our numerical method. The case in which a black hole becomes extremal is also beyond the scope of this method. Stability of extremal black holes may be very different from that of non-ex-

tremal black holes. There is a universal "horizon instability" [80–82]. We leave these issues to further studies.

We point out several topics worthy of further investigations. Stability with respect to massive perturbations should be explored in detail to reveal how the mass term affects stability with respect to charged perturbations. The stability of the 4D charged Einstein-Gauss-Bonnet anti de-Sitter black hole would be a very interesting issue to address as well. We plan to explore these questions in the near future.

ACKNOWLEDGMENTS

We thank Peng-Cheng Li, Minyong Guo, and Shao-Jun Zhang for helpful discussions. Peng Liu would like to thank Yun-Ha Zha for her kind encouragement during this work.

References

- [1] D. Lovelock, *J. Math. Phys.* **12**, 498-501 (1971)
- [2] T. Clifton, P. G. Ferreira, A. Padilla *et al.*, *Phys. Rept.* **513**, 1 (2012), arXiv:1106.2476[astro-ph.CO]
- [3] D. Glavan and C. Lin, *Phys. Rev. Lett.* **124**(8), 081301 (2020), arXiv:1905.03601[gr-qc]
- [4] P. G. S. Fernandes, *Phys. Lett. B* **805**, 135468 (2020), arXiv:2003.05491[gr-qc]
- [5] A. Casalino, A. Colleaux, M. Rinaldi *et al.*, *Regularized Lovelock gravity*, arXiv:2003.07068[gr-qc]
- [6] R. A. Konoplya and A. Zhidenko, *Phys. Rev. D* **101**(8), 084038 (2020), arXiv:2003.07788[gr-qc]
- [7] R. A. Konoplya and A. Zhidenko, *BTZ black holes with higher curvature corrections in the 3D Einstein-Lovelock theory*, arXiv:2003.12171[gr-qc]
- [8] S. Nojiri and S. D. Odintsov, *EPL* **130**(1), 10004 (2020), arXiv:2004.01404
- [9] S.-W. Wei and Y.-X. Liu, *Testing the nature of Gauss-Bonnet gravity by four-dimensional rotating black hole shadow*, arXiv:2003.07769[gr-qc]
- [10] R. Kumar and S. G. Ghosh, *JCAP* **07**(07), 053 (2020), arXiv:2003.08927[gr-qc]
- [11] S. G. Ghosh and S. D. Maharaj, *Phys. Dark Univ.* **30**, 100687 (2020), arXiv:2003.09841[gr-qc]
- [12] S. G. Ghosh and R. Kumar, *Generating black holes in the novel 4D Einstein-Gauss-Bonnet gravity*, arXiv:2003.12291[gr-qc]
- [13] D. V. Singh, S. G. Ghosh, and S. D. Maharaj, *Clouds of string in 4D novel Einstein-Gauss-Bonnet black holes*, arXiv:2003.14136[gr-qc]
- [14] A. Kumar and S. G. Ghosh, *Hayward black holes in the novel 4D Einstein-Gauss-Bonnet gravity*, arXiv:2004.01131[gr-qc]
- [15] A. Kumar and R. Kumar, *Bardeen black holes in the novel 4D Einstein-Gauss-Bonnet gravity*, arXiv:2003.13104[gr-qc]
- [16] D. D. Doneva and S. S. Yazadjiev, *Relativistic stars in 4D Einstein-Gauss-Bonnet gravity*, arXiv:2003.10284[gr-qc]
- [17] P. Liu, C. Niu, Xiaobao Wang *et al.*, *Traversable Thin-shell Wormhole in the Novel 4D Einstein-Gauss-Bonnet Theory*, arXiv:2004.14267[gr-qc]
- [18] T. Kobayashi, *JCAP* **07**, 013 (2020), arXiv:2003.12771[gr-qc]
- [19] H. Lu and Y. Pang, *Phys. Lett. B* **809**, 135717 (2020), arXiv:2003.11552
- [20] P. G. S. Fernandes, P. Carrilho, T. Clifton *et al.*, *Phys. Rev. D* **102**(2), 024025 (2020), arXiv:2004.08362
- [21] Robie A. Hennigar, David Kubiznak, and Robert B. Mann, *JHEP* **07**, 027 (2020), arXiv:2004.09472[gr-qc]
- [22] W. Y. Ai, *Commun. Theor. Phys.* **72**(9), 095402 (2020), arXiv:2004.02858
- [23] K. Aoki, M. Ali Gorji, and S. Mukohyama, *Consistent theory of $D \rightarrow 4$ Einstein-Gauss-Bonnet gravity*, arXiv:2005.03859[gr-qc]
- [24] R. A. Konoplya and A. F. Zinhailo, *Quasinormal modes, stability and shadows of a black hole in the novel 4D*

- [25] Einstein-Gauss-Bonnet gravity, arXiv: 2003.01188[gr-qc]
R. A. Konoplya and A. Zhidenko, *Phys. Dark Univ.* **30**, 100697 (2020), arXiv:2003.12492[gr-qc]
- [26] R. A. Konoplya and A. F. Zinhailo, *Grey-body factors and Hawking radiation of black holes in 4D Einstein-Gauss-Bonnet gravity*, arXiv: 2004.02248[gr-qc]
- [27] M. S. Churilova, *Quasinormal modes of the Dirac field in the novel 4D Einstein-GaussBonnet gravity*, arXiv: 2004.00513[gr-qc]
- [28] A. K. Mishra, *Quasinormal modes and Strong Cosmic Censorship in the novel 4D EinsteinGauss-Bonnet gravity*, arXiv: 2004.01243[gr-qc]
- [29] S. L. Li, P. Wu, and H. Yu, *Stability of the Einstein Static Universe in 4D Gauss-Bonnet Gravity*, arXiv: 2004.02080[gr-qc]
- [30] A. Aragón, R. Bécar, P. A. González *et al.*, *Perturbative and nonperturbative quasinormal modes of 4D Einstein-Gauss-Bonnet black holes*, arXiv: 2004.05632[gr-qc]
- [31] S.-J. Yang, J.-J. Wan, J. Chen *et al.*, *Weak cosmic censorship conjecture for the novel 4D charged Einstein-Gauss-Bonnet black hole with test scalar field and particle*, arXiv: 2004.07934
- [32] P. Liu, C. Niu, and C.-Y. Zhang, *Instability of the Novel 4D Charged Einstein-Gauss-Bonnet Anti de-Sitter Black Hole*, arXiv: 2005.01507[gr-qc]
- [33] C. Y. Zhang, P. C. Li, and M. Guo, *Greybody factor and power spectra of the Hawking radiation in the 4D Einstein-Gauss-Bonnet de-Sitter gravity*, accepted by EPJC. arXiv: 2003.13068
- [34] C. Y. Zhang, P. C. Li, and M. Guo, *JHEP* **2008**, 105 (2020), arXiv:2004.03141
- [35] M. A. Cuyubamba, *Stability of asymptotically de Sitter and anti-de Sitter black holes in 4D regularized Einstein-Gauss-Bonnet theory*, arXiv: 2004.09025[gr-qc]
- [36] M. Guo and P. C. Li, *Eur. Phys. J. C* **80**(6), 588 (2020), arXiv:2003.02523[gr-qc]
- [37] M. Heydari-Fard, M. Heydari-Fard, and H. R. Sepangi, *Bending of light in novel 4D GaussBonnet-de Sitter black holes by Rindler-Ishak method*, [arXiv: 2004.02140[gr-qc]]
- [38] X. h. Jin, Y.-x. Gao, and D. j. Liu, *Int. J. Mod. Phys. D* **29**(09), 2050065 (2020), arXiv:2004.02261[gr-qc]
- [39] Y. P. Zhang, S. W. Wei, and Y. X. Liu, *Universe* **6**(8), 103 (2020), arXiv:2003.10960[gr-qc]
- [40] S. U. Islam, R. Kumar, and S. G. Ghosh, *Gravitational lensing by black holes in 4D4D Einstein-Gauss-Bonnet gravity*, arXiv: 2004.01038[gr-qc]
- [41] J. Rayimbaev, A. Abdujabbarov, B. Turimov *et al.*, *Magnetized particle motion around 4-D Einstein-Gauss-Bonnet Black Hole*, arXiv: 2004.10031[gr-qc]
- [42] K. Hegde, A. N. Kumara, C. L. A. Rizwan *et al.*, *Thermodynamics, Phase Transition and Joule Thomson Expansion of novel 4-D Gauss Bonnet AdS Black Hole*, arXiv: 2003.08778[gr-qc]
- [43] S. W. Wei and Y. X. Liu, *Phys. Rev. D* **101**(10), 104018 (2020), arXiv:2003.14275[gr-qc]
- [44] D. V. Singh and S. Siwach, *Phys. Lett. B* **808**, 135658 (2020), arXiv:2003.11754
- [45] S. A. Hosseini Mansoori, *Thermodynamic geometry of novel 4-D Gauss Bonnet AdS Black Hole*, arXiv: 2003.13382[gr-qc]
- [46] B. Eslam Panah and Kh. Jafarzade, *4D Einstein-Gauss-Bonnet AdS Black Holes as Heat Engine*, arXiv: 2004.04058[hep-th]
- [47] S. Ying, *Thermodynamics and Weak Cosmic Censorship Conjecture of 4D Gauss-BonnetMaxwell Black Holes via Charged Particle Absorption*, arXiv: 2004.09480[gr-qc]
- [48] D. Malafarina, B. Toshmatov, and N. Dadhich, *Phys. Dark Univ.* **30**, 100598 (2020), arXiv:2004.07089[gr-qc]
- [49] C. Liu, T. Zhu, and Q. Wu, *Thin Accretion Disk around a four-dimensional Einstein-GaussBonnet Black Hole*, arXiv: 2004.01662[gr-qc]
- [50] A. Naveena Kumara, C. L. Ahmed Rizwan, K. Hegde *et al.*, *Rotating 4D Gauss-Bonnet black hole as particle accelerator*, arXiv: 2004.04521[gr-qc]
- [51] F.-W. Shu, *Vacua in novel 4D Einstein-Gauss-Bonnet Gravity: pathology and instability*, arXiv: 2004.09339[gr-qc]
- [52] K. Aoki, M. A. Gorji, and S. Mukohyama, *A consistent theory of $D \rightarrow 4$ EinsteinGaussBonnet gravity*, [arXiv: 2005.03859[gr-qc]]
- [53] K. Aoki, M. A. Gorji, and S. Mukohyama, *Cosmology and gravitational waves in consistent $D \rightarrow 4$ Einstein-Gauss-Bonnet gravity*, arXiv: 2005.08428 [gr-qc]
- [54] R. G. Cai, L. M. Cao, and N. Ohta, *JHEP* **104**, 082 (2010), arXiv:0911.4379
- [55] Y. Tomozawa, *Quantum corrections to gravity*, arXiv: 1107.1424[gr-qc]
- [56] G. Cognola, R. Myrzakulov, L. Sebastiani *et al.*, *Phys. Rev. D* **88**, 024006 (2013), arXiv:1304.1878
- [57] R. A. Konoplya and A. Zhidenko, *Rev. Mod. Phys.* **83**, 793-836 (2011), arXiv:1102.4014[gr-qc]
- [58] E. Berti, V. Cardoso, and A. O. Starinets, *Class. Quant. Grav.* **26**, 163001 (2009), arXiv:0905.2975[gr-qc]
- [59] C. Y. Zhang, S. J. Zhang, and B. Wang, *J. High Energy Phys.* **08**, 011 (2014), arXiv:1405.3811
- [60] V. Cardoso, J. a. L. Costa, K. Destounis *et al.*, *Phys. Rev. Lett.* **120**(3), 031103 (2018), arXiv:1711.10502
- [61] Y. Mo, Y. Tian, B. Wang *et al.*, *Phys. Rev. D* **98**, 124025 (2018), arXiv:1808.03635[gr-qc]
- [62] H. Liu, Z. Tang, K. Destounis *et al.*, *JHEP* **03**, 187 (2019), arXiv:1902.01865[gr-qc]
- [63] H. Zhang and Z. Zhong, *Strong cosmic censorship in de Sitter space: As strong as ever*, arXiv: 1910.01610[hep-th]
- [64] R. A. Konoplya and A. Zhidenko, *Phys. Rev. Lett.* **103**, 161101 (2009), arXiv:0809.2822[hep-th]
- [65] R. A. Konoplya and A. Zhidenko, *Phys. Rev. D* **89**(2), 024011 (2014), arXiv:1309.7667[hep-th]
- [66] M. A. Cuyubamba, R. A. Konoplya, and A. Zhidenko, *Phys. Rev. D* **93**(10), 104053 (2016), arXiv:1604.03604[gr-qc]
- [67] P.-C. Li, C.-Y. Zhang, and B. Chen, *JHEP* **1911**, 042 (2019), arXiv:1909.02685[hep-th]
- [68] C. Y. Zhang, S. J. Zhang, D. C. Zou *et al.*, *Phys. Rev. D* **93**(6), 064036 (2016), arXiv:1512.06472[gr-qc]
- [69] Z. Zhu, S.-J. Zhang, C. E. Pellicer *et al.*, *Phys. Rev. D* **90**(4), 044042 (2014), Addendum: *Phys. Rev. D* **90**(4), 049904 (2014), arXiv: 1405.4931 [hep-th]
- [70] R. A. Konoplya and A. Zhidenko, *Phys. Rev. D* **90**, 064048 (2014), arXiv:1406.0019[hep-th]
- [71] K. Destounis, *Phys. Rev. D* **100**(4), 044054 (2019), arXiv:1908.06117[gr-qc]
- [72] R. Brito, V. Cardoso, and P. Pani, *Lect. Notes Phys.* **906**, 1-237 (2015), arXiv:1501.06570[gr-qc]
- [73] C. Y. Zhang, S. J. Zhang, and B. Wang, *Nucl. Phys. B* **899**, 37 (2015), arXiv:1501.03260
- [74] H. T. Cho, A. S. Cornell, J. Doukas *et al.*, *Class. Quant. Grav.* **27**, 155004 (2010), arXiv:0912.2740
- [75] H. T. Cho, A. S. Cornell, J. Doukas *et al.*, *Adv. Math. Phys.* **2012**, 281705 (2012), arXiv:1111.5024[gr-qc]
- [76] R. L. H. H. Ciftci and N. Saad, *Journal of Physics A* **36**(47), 11807-11816 (2003), arXiv:math-ph/0309066
- [77] R. L. H. H. Ciftci, and N. Saad, *Physics Letters A* **340**(5-6), 388-396 (2005), arXiv:math-ph/0504056
- [78] K. A. Bronnikov, R. A. Konoplya, and A. Zhidenko, *Phys. Rev. D* **86**, 024028 (2012), arXiv:1205.2224]
- [79] R. Gregory and R. Laflamme, *Phys. Rev. Lett.* **70**, 2837-2840 (1993), arXiv:hep-th/9301052[hep-th]
- [80] S. Aretakis, *J. Funct. Anal.* **263**, 2770 (2012), arXiv:1110.2006[gr-qc]
- [81] S. Aretakis, *Adv. Theor. Math. Phys.* **19**, 507-530 (2015), arXiv:1206.6598[gr-qc]
- [82] S.-J. Zhang, Q. Pan, B. Wang *et al.*, *JHEP* **1309**, 101 (2013), arXiv:1308.0635[hep-th]